Proximate Quantum Spin Liquid on Designer Lattice

Xiaoran Liu[1],* Sobhit Singh[1], Victor Drouin-Touchette[1], T. Asaba[2], Jess H. Brewer[3,4], Qinghua Zhang[5], Yanwei Cao[6], B. Pal[1,7], S. Middey[8], P. S. Anil Kumar[8], M. Kareev[1], Lin Gu[5], D. D. Sarma[7], P. Shafer[9], E. Arenholz[9], J. W. Freeland[10], Lu Li[2], D. Vanderbilt[1], and J. Chakhalian[1]

[1] *Department of Physics and Astronomy, Rutgers University, Piscataway, New Jersey 08854, USA*
[2] *Department of Physics, University of Michigan, Ann Arbor, Michigan 48109, USA*
[3] *TRIUMF, 4004 Wesbrook Mall, Vancouver, British Columbia, Canada V6T 2A3*
[4] *Department of Physics and Astronomy, University of British Columbia, Vancouver, British Columbia, Canada V6T 1Z1*
[5] *Beijing National Laboratory for Condensed-Matter Physics and Institute of Physics, Chinese Academy of Sciences, Beijing 100190, P. R. China*
[6] *Ningbo Institute of Materials Technology and Engineering, Chinese Academy of Science, Ningbo, Zhejiang 315201, P. R. China*
[7] *Department of Solid State and Structural Chemistry Unit, Indian Institute of Science, Bengaluru 560012, India*
[8] *Department of Physics, Indian Institute of Science, Bengaluru , 560012, India*
[9] *Advanced Light Source, Lawrence Berkeley National Laboratory, Berkeley, California 94720, USA and*
[10] *Advanced Photon Source, Argonne National Laboratory, Argonne, Illinois 60439, USA*

(Dated: May 25, 2020)

Complementary to bulk synthesis, here we propose a generic designer lattice with extremely high magnetic frustration, and demonstrate the possible realization of a quantum spin liquid phase from both experiments and theoretical calculations. In an ultrathin (111) $CoCr_2O_4$ slice composed of three triangular and one kagome cation planes, the absence of a spin ordering transition is demonstrated down to 0.03 K, in the presence of strong antiferromagnetic correlation in the energy scale of 30 K between Co and Cr sublattices. Freezing of spins is excluded and persisting spin fluctuations are observed at low temperatures via muon spin relaxation. Our calculations further demonstrate the existence of highly degenerate magnetic ground states at the 0 K limit, due to the competition among multiple exchange interactions. These results collectively indicate the realization a proximate quantum spin liquid state on the designer lattice.

In a magnetic crystal the basic notion of minimizing free energy necessitates that after cooling down to sufficiently low temperature all spins should lock into a long-range ordered pattern. However, on a lattice where the exchange interactions between localized spins cannot be simultaneously satisfied, the system becomes magnetically frustrated, with the tendency of forming unusual disordered magnetic phases significantly different from a simple paramagnet [1]. Furthermore, from a theory standpoint, the combination of electronic correlations, quantum fluctuations, spin-orbit couplings, and lattices supporting frustrated magnetic interactions has been a remarkably fertile ground for predicting unconventional entangled states of quantum matter including spin ice, topological superconductor, axion insulator, Weyl semimetal, magnetic monopole, and a variety of liquid-like spin states [2–10]. A quantum spin liquid (QSL) belongs to one of these exotic states; generally, it possesses no long-range magnetic order, lacks any spontaneously broken symmetry, and carries a spectrum of fractional excitations [11–14].

As for the experimental realization of a QSL, the currently existing recipes are illuminating but limited [15–21]. On the one hand, a general guiding principle is that, in order to reach a QSL, significant frustration resulting either from the lattice geometry, multiple exchange terms, or bond conflict is an important prerequisite [18]. After tremendous decades-long efforts promising candidate materials have been identified and synthesized, including the prototypical instances of the widely studied organic salts $EtMe_3Sb[Pd(dmit)_2]_2$ and κ-$(ET_2)Cu_2(CN)_3$, the herbertsmithite $ZnCu_3(OH)_6Cl_2$ and barlowite $Cu_3Zn(OH)_6FBr$, and the Kitaev magnets with QSLs α-$RuCl_3$ and A_2IrO_3 (A = Na, Li) [18]. It is worth noting, however, the underlying lattices of almost all QSL candidates are mainly bound to five types of lattice geometries, namely, triangular, pyrochlore, kagome, hyperkagome, and honeycomb lattices [11, 17, 20]. This in turn seems to limit the pursuit of additional QSL candidates, and brings to the focus an open question of whether any additional type of lattice can support a QSL and how can it be achieved experimentally.

In recent years, complementary to bulk synthesis, heteroepitaxial engineering of ultrathin films, multilayers and superlattices by means of advanced deposition techniques has been developed into a powerful platform for materials design and innovation [22–28]. In particular, geometrical lattice engineering principally aiming at the design and fabrication of lattices with artificial geometry by stacking on demand a specific number of atomic planes along unconventional crystallographic directions has been recognized as a promising path to emergent phenomena [29–35]. This framework once experimentally validated can offer an alternative approach to create new types of synthetic lattices potentially hosting QSL and other interesting states of quantum matter.

In this Letter, to address these challenges, we propose a generic design of a novel quasi-two-dimensional (quasi-2D) lattice derived from the normal spinel structure, and demonstrate its feasibility for supporting a QSL phase from both advanced experiments and theoretical calculations. Concretely, using $CoCr_2O_4$ as a prototype, we fabricated a series of (111)-

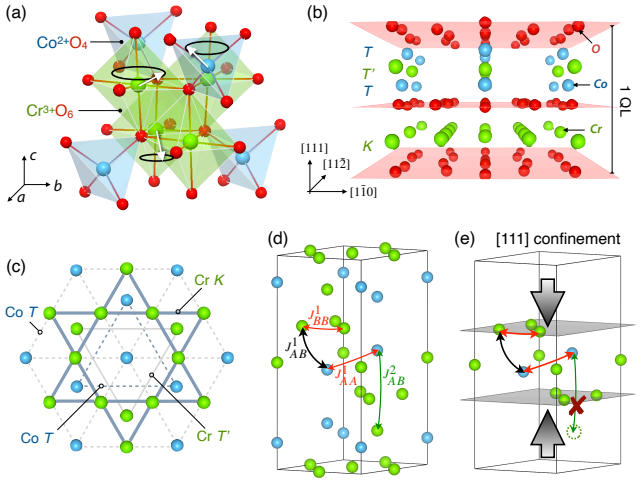

FIG. 1. (a) Schematic representation of bulk $CoCr_2O_4$ composed of networks of $Co^{2+}O_4$ tetrahedra and $Cr^{3+}O_6$ octahedra. The arrows depict the conical spin configuration of the ground state. (b) Definition of one quadruplet layer (1 QL) of $CoCr_2O_4$ along the [111] direction, including four alternative cation planes: kagome Cr plane (K), triangle Co plane (T), triangle Cr plane (T′), and triangle Co plane (T). (c) [111] top view of the alternative cation planes in 1 QL. (d) Magnetic exchange pathways in (111) $CoCr_2O_4$. (e) Effects of [111] confinement on the exchange couplings in 1 QL $CoCr_2O_4$.

oriented ultrathin films, confined by nonmagnetic Al_2O_3 layers into a quantum well geometry. Compared to its bulk counterpart, the onset of the ferrimagnetic transition decreases monotonically with reduced thickness, and eventually shuts off in a single unit slab of (111) $CoCr_2O_4$; In this quasi-2D limit, the degree of magnetic frustration is enhanced by almost three orders of magnitude. Our first-principles density-functional theory (DFT) calculations and classical Monte-Carlo (MC) simulations on this designer lattice further reveal the presence of strongly frustrated magnetic configurations with a tremendous degree of degeneracy, which prevents the system from achieving a definite magnetic order at ultra low temperatures. These combined results imply the realization of a proximate QSL in the single unit (111) $CoCr_2O_4$ slice.

$CoCr_2O_4$ belongs to the normal spinel (AB_2O_4) chromite family, MCr_2O_4 (M = Mn, Fe, Co and Ni) [36], where the magnetically active M^{2+} ions occupy the tetrahedral A sites of diamond sublattice and the Cr^{3+} ions occupy the octahedral B sites of pyrochlore sublattice, possessing complex spin configuration of the ground state [37]. Specifically, in bulk $CoCr_2O_4$ [Fig. 1(a)], a collinear ferrimagnetic state first forms with the Curie temperature of ∼93 K, which transforms into an incommensurate spiral ferrimagnetic state at ∼26 K. An incommensurate to commensurate lock-in transition further takes place at ∼14 K [38, 39]. When viewed along the [111] direction, the structure is an intrinsic stacking of triangle and kagome cation planes from Co and Cr ions embedded in the oxygen cubic close-packed frame. This leads to a sequence of "– O – Cr(K) – O – Co(T) – Cr(T′) – Co(T) –" in a single unit with four cation atomic layers, which we denote as one quadruplet layer (1 QL) [Fig. 1(b)-(c)].

Bulk $CoCr_2O_4$ is weakly frustrated due to the interplay of multiple exchange couplings [Fig. 1d]. The most dominant first-neighbor J^1_{AB} inter-atomic coupling is antiferromagnetic (AFM), which alone would favor a Néel-type collinear ferrimagnetic ordering. The weak magnetic frustration originates from the competition between J^1_{AB} and the intra-atomic AFM couplings J^1_{BB} and J^1_{AA}, and is partially relieved by the second-neighbor ferromagnetic coupling J^2_{AB}. Based on the entwined nature of those couplings, we can conjure that if the lattice is made [111] confined, the magnetic frustration could be markedly elevated as a result of enhanced geometric frustration from J^1_{BB} and J^1_{AA} on kagome and triangle planes plus termination of the out-of-plane J^2_{AB}, which may collectively trigger the formation of QSL.

Based on this design idea, ultrathin films of n QL $CoCr_2O_4$ (n = 1, 2, 4; 1 QL ∼4.8 Å) confined by Al_2O_3 quantum wells (∼13 Å) were fabricated by pulsed laser deposition on (0001)-oriented single crystal Al_2O_3 substrates. Details of the synthesis and characterization were reported elsewhere [40, 41]. It is worth noting, recently, we discovered an emergent Yafet-Kittel type ferrimagnetic state in 4 and 2 QL $CoCr_2O_4$ due to enhanced frustration [35]. In this Letter, we primarily focus on the 1 QL case.

First, we start with the investigation of the magnetic behavior of each sublattice by recording the resonant x-ray absorption spectra (XAS) taken with left- and right-circularly polarized x-ray beams. The difference between those two spectra, namely, x-ray magnetic circular dichroism (XMCD) reflects the net magnetization of a specifically probed element [42]. As shown in Fig. 2(a), XMCD of both Cr and Co are clearly observed at 15 K with opposite sign, as indicated by the distinct features at L_3 edges (Cr ∼577 eV and Co ∼778 eV). These results confirm that at low temperatures due to the AFM J^1_{AB} term, the overall orientation of spins on the Co sublattice is along the field, whereas that on the Cr sublattice against. Then at high temperatures where the thermal energy overcomes the exchange interaction, a paramagnetic state is expected such that the orientation of all spins should be aligned parallel to the external field. This is in fact demonstrated by temperature-dependent XMCD spectra at L_3 edges, where the sign of Cr flips at temperatures above ∼30 K [see Fig. 2(d)].

With the knowledge about the scale of J^1_{AB}, we can explore whether a long-range magnetic ordering is presents in 1 QL $CoCr_2O_4$. The J^1_{AB} term alone favors a ferrimagnetic state, with a ferromagnetic spin arrangement on each sublattice [43]. As a result, hysteretic behavior is anticipated from field-dependent XMCD scans. As seen in Fig. 2(b), this is indeed observed in the thicker 4 QL $CoCr_2O_4$ that exhibits clear hysteresis loops at both Co and Cr L_3 edges, consistent with the previous study that the ground state of 4 QL $CoCr_2O_4$ hosts an emergent Yafet-Kittel type ferrimagnetic ordering [35]. However, in sharp contrast, no hysteresis loop but a linear XMCD vs. H relationship is found on both elements in 1 QL $CoCr_2O_4$, typical of a paramagnetic behavior.

In order to further examine if any long-range spin order-

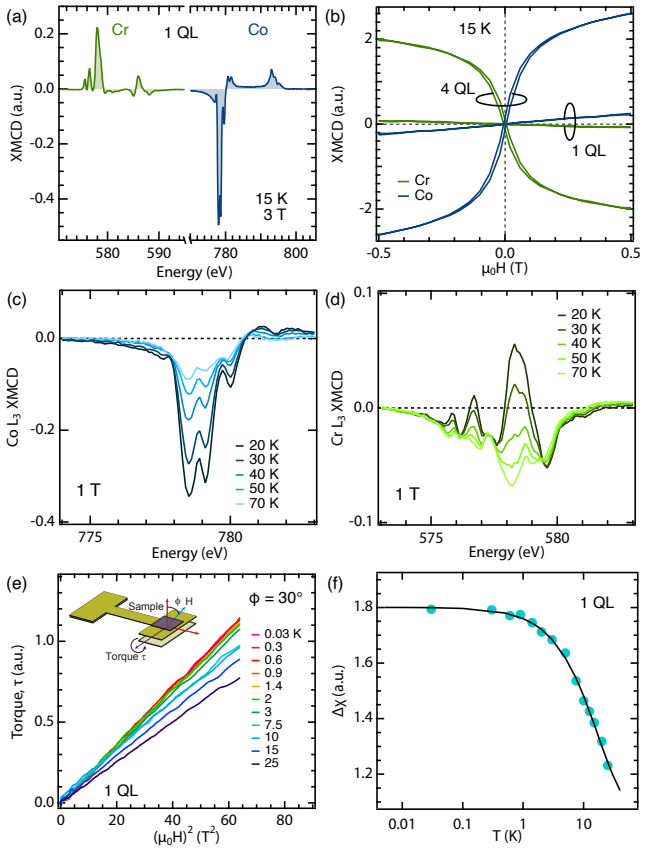

FIG. 2. (a) XMCD spectra at $L_{2,3}$ edges of both Co and Cr in 1 QL $CoCr_2O_4$. (b) Field dependence of the XMCD L_3 intensity of Co ($\sim$ 778 eV) and Cr ($\sim$ 577 eV). Results of both 4 and 1 QL $CoCr_2O_4$ are shown for comparison. (c)-(d) Co and Cr L_3 XMCD spectra at various temperatures. (e) Torque magnetometry curves of 1 QL $CoCr_2O_4$ at various temperatures between 25 – 0.03 K. (f) Temperature dependence of $\Delta\chi$ extracted from linear fit of the τ vs. H^2 curves [$\tau = \Delta\chi(\mu_0 H)^2$] from (e).

ing emerges at extremely low temperatures, we performed the torque magnetometry measurements on 1 QL $CoCr_2O_4$ from 30 K down to 0.03 K. This technique quantifies the magnetic torque response of a sample with respect to the applied magnetic field ($\tau \propto \mathbf{M} \times \mathbf{H}$), and has been demonstrated an exquisitely sensitive utility to probe vanishingly small magnetic signals from ultrathin samples and interfaces [44, 45]. The result shown in Fig. 2(e) confirms that within the resolution of measurement and entire temperature range, no hysteresis but a reversible parabolic $\tau \propto (\mu_0 H)^2$ relationship is observed, which implies a paramagnetic behavior persisting down to 0.03 K. Note, to make a thorough comparison and eliminate any question about sensitivity of measurement, we collected the torque signal of 4 QL $CoCr_2O_4$ using the same geometry. The data clearly exhibit distinct hysteretic loops below the Curie temperature of 58 K, a hallmark of ferro-/ferri-magnetism [see the Supplemental, Fig.3]. These observations agree well with the field-dependent XMCD results, providing strong evidence for the absence of long-range magnetic ordering in 1 QL $CoCr_2O_4$ down to 0.03 K. Combination of these results leads to an extremely large frustration factor $f = \theta_{CW}/T_c \sim$1000 in 1 QL, almost three orders of magnitude compared to that ($f \sim$6) in bulk $CoCr_2O_4$ [46]. Furthermore, it is notable that the extracted anisotropic susceptibility $\Delta\chi$ smoothly increases as the temperature decreases and becomes essentially non-zero and temperature-independent below $\sim$1 K, as indicated by the solid line in Fig. 2f. These provide strong support for the existence of low-lying magnetic excitations, implying the nearly degenerate ground states of 1 QL [47].

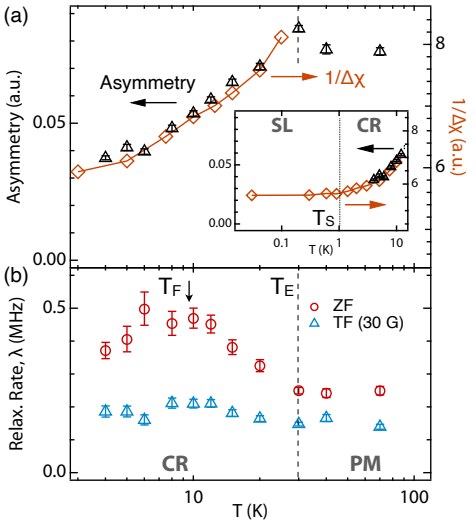

FIG. 3. (a) Temperature dependence of the spin asymmetry (left axis) from μ^+ decay and $1/\Delta\chi$ (right axis) from torque measurements on 1 QL $CoCr_2O_4$. The inset shows the data at 0.03 – 10 K, with T_S indicating the temperature-independent behavior of $1/\Delta\chi$ below $\sim$1 K. (b) Temperature dependence of the μ^+ spin relaxation rate λ from both zero field (red) and 30 G transverse field (blue) measurements. Both asymmetry and λ shows a temperature-independent behavior above $T_E \sim$30 K; Below 30 K, λ gradually increases to a broad peak at $T_F \sim$10 K. PM, CR, and SL represent 'paramagnet', 'crossover region', and 'spin liquid', respectively.

Next, we turn to investigate the spin dynamics of 1 QL $CoCr_2O_4$ by muon spin relaxation (μSR) spectroscopy in both zero-field (ZF) and 30 G transverse-field (TF) setup. Thanks to its high sensitivity to local fields and capability to characterize their timescale of fluctuations, μSR has been prominently applied on materials without long-range magnetic ordering [48–57]. In ZF-μSR, a simple exponential decay with no oscillatory signal is observed, while a slowly relaxing signal precessing at the muon Larmor frequency is clearly observed in all of the TF-μSR spectra (for representative data at 20 K see the Supplemental Fig.4). As a result, no coherent precession of the incident μ^+ is found, ruling out the formation of a static uniform local field, characteristic of magnetic phases without long-range order (i.e. ferro-/ferri-magnet and commensurate antiferromagnet) [49].

The spin asymmetry and the spin relaxation rate λ are extracted by fitting the spectra of the time evolution of polariza-

tion [see Supplemental for more details], and their temperature dependencies are shown in Fig. 3. While below 30 K, the asymmetry decreases with the lowered temperatures, both relaxation rates (in ZF and TF) first increase, reaching a broad "hump" at around 10 K, followed by a reduction again at the base temperatures. These results deem a spin glass transition to be absent because: (1) The simple exponential relaxation observed at all temperatures is not the expected form for any type of spin glass [58, 59]; (2) In addition, the ZF-μSR time spectra lack the "tail" of polarization recovery to 1/3, which is expected in spin glasses with static random local fields [49]; (3) the ZF λ only slightly increases from ~0.25 MHz at 70 K to 0.35 MHz at 4 K, while below the freezing point of a spin glass, λ typically increases by an order of magnitude ($\lambda \sim$ 1-20 MHz) [53].

From the spin dynamics viewpoint, three characteristic temperatures, T_E, T_F, and T_S appear on 1 QL $CoCr_2O_4$. Specifically, above T_E ~30 K, the muon spins are mainly depolarized by the rapid fluctuations of local fields due to thermal excitations, leading to both asymmetry and λ nearly constant, which are conventional paramagnetic features. This observation is consistent with the XMCD results, which indicate the thermal energy overcomes the most dominant J^1_{AB} at 30 K. Next, asymmetry starts to decrease accompanied by the increase in λ suggesting the slowing down of spin fluctuations in some fraction of sample due to the onset of J^1_{AB}, triggering short-range spin-spin correlations between Co and Cr ions. We recap that the local moments of both Co^{2+} (S = 3/2) and Cr^{3+} (S = 3/2) are ~3.7 μ_B, which should correspond to a local distribution ~4500 G for a fully static spin [60]. However, we observed a field of only ~500 G, which corresponds to a static moment ~0.4 μ_B only. This indicates that the majority of the Co and Cr moments do not freeze and remain fluctuating at finite frequency down to 4 K.

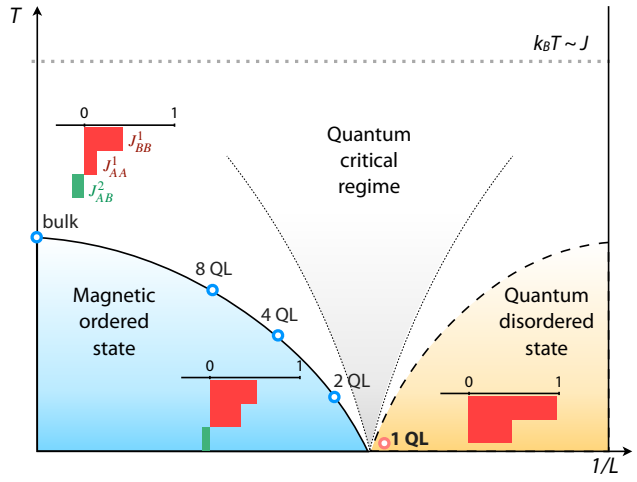

FIG. 4. Evolution of the magnetic states of n QL $CoCr_2O_4$ mapped onto a generic diagram of the quantum phase transition. L refers to the out-of-plane dimension. For bulk, $n = 2$, and $n = 1$, the normalized strength of each exchange coupling (J^N_{ij} / J^1_{AB}) is exhibited by the bar chart; red (green) color indicates AFM (FM) coupling.

At this point we compare $\Delta\chi$ deduced from the torque data to the local spin susceptibility sensed by muons. As seen in Fig. 3(a), the trend of asymmetry closely resembles that of the inverse $\Delta\chi$. Namely, it monotonically drops to about 50% at 4 K and possibly becomes temperature-independent below T_S ~1 K. Thus, we conjecture that below 1 K, the spins are entangled all over the sample with the persisting spectrum of fluctuations. On the other hand, the relaxation rates reach a "hump" at T_F ~10 K but drop to finite values at low temperatures. This is another strong evidence for the absence of conventional orderings, where $\lambda \to 0$ at $T \to 0$ reflecting the freezing out of magnetic excitations [60].

To obtain a microscopic insight into how the designer lattice topology and quantum confinement alter the exchange interactions and consequently the magnetic ground state, we performed DFT calculations and MC simulations on bulk, 2 and 1 QL $CoCr_2O_4$. We calculate the normalized strength of each exchange term J^N_{ij}/J^1_{AB}. As shown in Fig. 4, towards the 2D limit, it is striking that the relative strengths of J^1_{BB} and J^1_{AA}, which act to enhance frustration, increase, whereas the contribution of J^2_{AB}, which tends to relieve frustration, decreases. The computational data reveal this key effect is a consequence of the markedly smaller number of second-neighbor interactions along (111) in the 2D limit compared to bulk. In fact, for 1 QL $CoCr_2O_4$ with J^2_{AB} completely terminated, J^1_{BB} and J^1_{AA} reach almost the same scale as J^1_{AB}. This trend agrees very well with the experiments, which evidently indicates the presence of extremely large magnetic frustration in 1 QL. Additionally, our classical MC simulations lends further support to this claim, affirming the presence of a paramagnetic phase with a plethora of competing magnetic ground states in 1 QL $CoCr_2O_4$ [Supplemental Figs.8-10].

Finally, we can map the ground state of the n QL $CoCr_2O_4$ system onto a generic quantum phase transition diagram [61]. In the bulk ($n \to \infty$), the ground state is a well-defined long-range magnetic ordered state. As n is reduced, it is more and more difficult to stabilize a conventional ordered state due to the enhancement of magnetic frustration. Eventually the ground state becomes highly degenerate in 1 QL $CoCr_2O_4$, unleashing dynamical spin fluctuations. We note this is the regime where quantum effects play a pivotal role and may bring the system into a proximate QSL state.

To summarize, we proposed a general design scheme for novel lattices supporting QSL, and revealed a possible realization in 1 QL $CoCr_2O_4$, where the magnetic frustration is profound and the ground state is highly degenerate with robust spin fluctuations. Our findings call for further investigation on the excitation spectrum and open a window to a broad class of synthetic QSL candidates.

ACKNOWLEDGMENTS

The authors deeply acknowledge D. Khomskii, G. Fiete, X. Hu, P. Coleman, K. Rabe, P. Chandra and P. Mahadevan for numerous insightful discussions, and A. Suter and P. Thomas

for their assistance on the μSR experiments. X.L. and J.C. acknowledge the support by the Gordon and Betty Moore Foundation EPiQS Initiative through Grant No. GBMF4534, and by the Department of Energy under Grant No. DE-SC0012375. The research of L.L. is supported by the US Department of Energy, Office of Basic Energy Sciences, Division of Materials Sciences and Engineering under Award DE-SC0008110 (high-field magnetization). This research used resources of the Advanced Light Source, which is a Department of Energy Office of Science User Facility under Contract No. DE-AC0205CH11231. This research used resources of the Advanced Photon Source, a U.S. Department of Energy Office of Science User Facility operated by Argonne National Laboratory under Contract No. DE-AC02-06CH11357.

* xiaoran.liu@rutgers.edu

[1] Ramirez, A. P. Strongly geometrically frustrated magnets. *Annu. Rev. Mater. Sci.* **24**, 453-480 (1994).
[2] P. Lee From high temperature superconductivity to quantum spin liquid: progress in strong correlation physics. *Rep. Prog. Phys.* **71**, 012501 (2008).
[3] Z. Y. Meng, T. C. Lang, S. Wessel, F. F. Assaad & A. Muramatsu Quantum spin liquid emerging in two-dimensional correlated Dirac fermions. *Nature* **464**, 847-851 (2010).
[4] F. L. Pratt, P. J. Baker, S. J. Blundell, T. Lancaster, S. Ohira-Kawamura, C. Baines, Y. Shimizu, K. Kanoda, I. Watanabe, G. Saito, *Nature* **471**, 612 (2011).
[5] H. Jiang, H. Yao & L. Balents Spin liquid ground state of the spin-1/2 square J1-J2 Heisenberg model. *Phys. Rev. B* **86**, 024424 (2012).
[6] J. Knolle, D. L. Kovrizhin, J. T. Chalker & R. Moessner Dynamics of a two-dimensional quantum spin liquid: signatures of emergent Majorana fermions and fluxes. *Phys. Rev. Lett.* **112**, 207203 (2014).
[7] Wilczek, F. Majorana returns. *Nat. Phys.* **5**, 614-618 (2009).
[8] Ross, K. A., Savary, L., Gaulin, B. D. & Balents, L. Quantum excitations in quantum spin ice. *Phys. Rev. X* **1**, 021002 (2011).
[9] C. Nisoli, R. Moessner, P. Schiffer, *Rev. Mod. Phys.* **85**, 1473 (2013).
[10] Witczak-Krempa, W., Chen, G., Kim, Y. & Balents, L. Correlated quantum phenomena in the strong spin-orbit regime. *Annu. Rev. Condens. Matter Phys.* **5**, 57-82 (2014).
[11] Balents, L. Spin liquids in frustrated magnets. *Nature* **464**, 199-208 (2010).
[12] Zhou, Y., Kanoda, K. & Ng, T. Quantum spin liquid states. *Rev. Mod. Phys.* **89**, 025003 (2017).
[13] Misguich, G. "Quantum spin liquids and fractionalization" in *Introduction to frustrated magnetism*, Lacroix, C., Mendels, P. & Mila, F. Eds. (Springer, Berlin, 2011), chap. 16.
[14] T. Imai & Y. S. Lee Do quantum spin liquids exist? *Phys. Today* **69**, 30 (2016).
[15] Patrick A. Lee An end to the drought of quantum spin liquids. *Science* **321**, 1306 (2008).
[16] M. R. Norman Colloquium: Herbertsmithite and the search for the quantum spin liquid. *Rev. Mod. Phys.* **88**, 041002 (2016).
[17] Savary, L. & Balents, L. Quantum spin liquids: a review. *Rep. Prog. Phys.* **80**, 016502 (2017).
[18] C. Broholm, R. J. Cava, S. A. Kivelson, D. G. Nocera, M. R. Norman, & T. Senthil Quantum spin liquids. *Science* **367**, 263 (2020).
[19] H. Takagi, T. Takayama, G. Jackeli, G. Khaliullin & S. E. Nagler Concept and realization of Kitaev quantum spin liquids *Nat. Rev. Phys.* **1**, 264-280 (2019).
[20] J. Wen, S. Yu, S. Li, W. Yu, & J. Li Experimental identification of quantum spin liquids. *npj Quantum Mater.* **4**, 12 (2019).
[21] Mila, F. Quantum spin liquids. *Eur. J. Phys.* **21**, 499-510 (2000).
[22] Schlom, D., Chen, L., Eom, C., Rabe, K., Streiffer, S. & Triscone, J. Strain Tuning of ferroelectric thin films. *Annu. Rev. Mater. Res.* **37**, 589-626 (2007).
[23] Zubko, P., Gariglio, S., Gabay, M., Ghosez, P. & Triscone, J. Interface physics in complex oxide heterostructures. *Annu. Rev. Condens. Matter Phys.* **2**, 141-65 (2011).
[24] Hwang, H. Y., Iwasa, Y., Kawasaki, M., Keimer, B., Nagaosa, N. & Tokura, Y. Emergent phenomena at oxide interfaces. *Nat. Mater.* **11**, 103-113 (2012).
[25] Chakhalian, J., Freeland, J. W., Millis, A. J., Panagopoulos, C. & Rondinelli J. M. Colloquium: Emergent properties in plane view: Strong correlations at oxide interfaces. *Rev. Mod. Phys.* **86**, 1189 (2014).
[26] Stemmer, S. & James Allen, S. Two-dimensional electron gases at complex oxide interfaces. *Annu. Rev. Mater. Res.* **44**, 151-71 (2014).
[27] Huang, Z., Ariando, Wang, X., Rusydi, A., Chen, J., Yang, H. & Venkatesan, T. Interface engineering and emergent phenomena in oxide heterostructures. *Adv. Mater.* **30**, 1802439 (2018).
[28] Ramesh, R. & Schlom, D. Creating emergent phenomena in oxide superlattices. *Nat. Rev. Mater.* **4**, 257-268 (2019).
[29] Ueda, K., Tabata, H. & Kawai, T. Ferromagnetism in $LaFeO_3$-$LaCrO_3$ superlattices. *Science* **280**, 1064 (1998).
[30] Gibert, M., Zubko, P., Scherwitzl, R., Iniguez, J. & Triscone, J. Exchange bias in $LaNiO_3$-$LaMnO_3$ superlattices. *Nat. Mater.* **11**, 195 (20 12).
[31] Liu, X., Middey, S., Cao, Y., Kareev, M. & Chakhalian, J. Geometrical lattice engineering of complex oxide heterostructures: a designer approach to emergent quantum states. *MRS communications* **6**, 133-144 (2016).
[32] Middey, S. *et al.* Mott electrons in an artificial graphenelike crystal of rare-earth nickelate. *Phys. Rev. Lett.* **116**, 056801 (2016).
[33] Kim, T. H. *et al.* Polar metals by geometric design. *Nature* **533**, 68-72 (2016).
[34] A. Arab *et al.* Electronic structure of a Graphene-like artificial crystal of $NdNiO_3$. *Nano Lett.* **19**, 8311-8317 (2019).
[35] Liu, X., Singh, S., Kirby, B. J., Zhong, Z., Cao, Y., Pal, B., Kareev, M., Middey, S., Freeland, J. W., Shafer, P., Arenholz, E., Vanderbilt, D., & Chakhalian, J. Emergent magnetic state in (111)-oriented quasi-two-dimensional spinel oxides. *Nano Lett.* **19**, 8381-8387 (2019).
[36] Mufti, N., Nugroho, A. A., Blake, G. R. & Palstra, T. T. M. Magnetodielectric coupling in frustrated spin systems: the spinels MCr_2O_4 (M = Mn, Co and Ni). *J. Phys.: Condens. Matter* **22**, 075 902 (2010).
[37] Lyons, D. H., Kaplan, T. A., Dwight, K. & Menyuk, N. Classical theory of the ground spin-state in cubic spinels. *Phys. Rev.* **126**, 540 (1962).
[38] Tomiyasu, K., Fukunaga, J. & Suzuki, K. Magnetic short-range order and reentrant-spin-glass-like behavior in $CoCr_2O_4$ and $MnCr_2O_4$ by means of neutron scattering and magnetization measurements. *Phys. Rev. B* **70**, 214434 (2004).
[39] Chang, L., Huang, D., Li, W.-H., Cheong, S.-W., Ratcliff, W. & Lynn, J. Crossover from incommensurate to commensurate

magnetic orderings in $CoCr_2O_4$. *J. Phys.: Condens. Matter* **21**, 456008 (2009).

[40] Xiaoran Liu, M. Kareev, Y. Cao, J. Liu, S. Middey, D. Meyers, J. W. Freeland, and J. Chakhalian. Electronic and magnetic properties of (111)-oriented $CoCr_2O_4$ epitaxial thin film. *Appl. Phys. Lett.* **105**, 042401 (2014).

[41] Xiaoran Liu, D. Choudhury, Y. Cao, S. Middey, M. Kareev, D. Meyers, J.-W. Kim, P. Ryan, and J. Chakhalian. Epitaxial growth of (111)-oriented spinel $CoCr_2O_4/Al_2O_3$ heterostructures. *Appl. Phys. Lett.* **106**, 071603 (2015).

[42] C. T. Chen, Y. U. Idzerda, H.-J. Lin, N. V. Smith, G. Meigs, E. Chaban, G. H. Ho, E. Pellegrin & F. Sette *Phys. Rev. Lett.* **75**, 152 (1995).

[43] Y. Yamasaki, S. Miyasaka, Y. Kaneko, J.-P. He, T. Arima, and Y. Tokura Magnetic reversal of the ferroelectric polarization in a multiferroic spinel oxice. *Phys. Rev. Lett.* **96**, 207204 (2006).

[44] Li, L. *et al.* Phase transitions of Dirac electrons in bismuth. *Science* **321**, 547-550 (2008).

[45] Li, L., Richter, C., Mannhart, J. & Ashoori, R. C. Coexistence of magnetic order and two-dimensional superconductivity at $LaAlO_3/SrTiO_3$ interfaces. *Nat. Phys.* **7**, 762-766 (2011).

[46] Tsurkan, V., Zherlitsyn, S., Yasin, S., Felea, V., Skourski, Y., Deisenhofer, J., Krug von Nidda, H.-A., Wosnitza, J. & Loidl, A. Unconventional magnetostructural transition in $CoCr_2O_4$ at high magnetic field. *Phys. Rev. Lett.* **110**, 115502 (2013).

[47] D. Watanabe, M. Yamashita, S. Tonegawa, Y. Oshima, H. M. Yamamoto, R. Kato, I. Sheikin, K. Behnia, T. Terashima, S. Uji, T. Shibauchi, and Y. Matsuda Novel Pauli-paramagnetic quantum phase in a Mott insulator. *Nat. Commun.* **3**, 1090 (2012).

[48] R. S. Hayano, Y. J. Uemura, J. Imazato, N. Nishida, T. Yamazaki & R. Kubo Zero- and low-field spin relaxation studied by positive muons. *Phys. Rev. B* **20**, 850 (1979).

[49] P. Dalmas de Reotier and A. Yaouanc Muon spin rotation and relaxation in magnetic materials. *J. Phys.: Condens. Matter* **9**, 9113-9166 (1997).

[50] M. Klanjsek et al. A high-temperature quantum spin liquid with polaron spins. *Nat. Phys.* **13**, 1130 (2017).

[51] Y. J. Uemura, T. Yamazaki, D. R. Harshman, M. Senba & E. J. Ansaldo Muon-spin relaxation in AuFe and CuMn spin glasses. *Phys. Rev. B* **31** 546 (1985).

[52] Y. J. Uemura, et al. Spin fluctuations in frustrated kagome lattice system SrCr8Ga4O19 studied by muon spin relaxation. *Phys. Rev. Lett.* **73**, 3306 (1994).

[53] Y. Li, D. Adroja, P. K. Biswas, P. J. Baker, Q. Zhang, J. Liu, A. A. Tsirlin, P. Gegenwart, and Q. Zhang Muon spin relaxation evidence for the U(1) quantum spin-liquid ground state in the triangular antiferromagnet $YbMgGaO_4$. *Phys. Rev. Lett.* **117**, 097201 (2016).

[54] G. M. Luke, A. Keren, L. P. Le, W. D. Wu, Y. J. Uemura, D. A. Bonn, L. Taillefer & J. D. Garrett Muon spin relaxation in UPt3. *Phys. Rev. Lett.* **71**, 1466 (1993).

[55] L. Chang, M. Lees, I. Watanabe, A. Hillier, Y. Yasui, & S. Onoda Static magnetic moments revealed by muon spin relaxation and thermodynamic measurements in the quantum spin ice Yb2Ti2O7. *Phys. Rev. B* **89**, 184416 (2014).

[56] L. Clark et al. *Phys. Rev. Lett.* **110**, 207208 (2013).

[57] O. Mustonen, S. Vasala, E. Sadrollahi, K. P. Schmidt, C. Baines, H. C. Walker, I. Terasaki, F. J. Litterst. E. Baggio-Saitovitch & M. Karppinen *Nature Commun.* **9**, 1085 (2018).

[58] J. C. Phillips Stretched exponential relaxation in molecular and electronic glasses. *Rep. Prog. Phys.* **59**, 1133-1207 (1996).

[59] Y. J. Uemura, T. Yamazaki, R. S. Hayano, R. Nakai, and C. Y. Huang. *Phys. Rev. Lett.* **45**, 583-587 (1980).

[60] M. T. Rovers, P. P. Kyriakou, H. A. Dabkowska, and G. M. Luke Muon-spin-relaxation investigation of the spin dynamics of geometrically frustrated chromium spinels. *Phys. Rev. B* **66**, 174434 (2002).

[61] M. Vojta Frustration and quantum criticality. *Rep. Prog. Phys.* **81**, 064501 (2018).